Jilin Daxue Xuebao (Gongxueban)/Journal of Jilin University (Engineering and Technology Edition)
ISSN: 1671-5497
E-Publication: Online Open Access
Vol: 43 Issue: 07-2024
DOI: 10.5281/zenodo.12793416

ADSORPTION STUDY OF Cu AND Pb HEAVY METALS FROM WATER SOLUTION USING $MnFe_2O_4$ AND $MnFe_2O_4$-Zeolite

RAMLAN
Department of Physics, Faculty of Natural Sciences, Sriwijaya University, Inderalaya, Ogan Ilir (OI). South Sumatera, Indonesia.

LUH AYU
Department of Physics, Faculty of Natural Sciences, Sriwijaya University, Inderalaya, Ogan Ilir (OI). South Sumatera, Indonesia.

AHKMAD AMINUDDIN BAMA
Department of Physics, Faculty of Natural Sciences, Sriwijaya University, Inderalaya, Ogan Ilir (OI). South Sumatera, Indonesia.

AKMAL JOHAN
Department of Physics, Faculty of Natural Sciences, Sriwijaya University, Inderalaya, Ogan Ilir (OI). South Sumatera, Indonesia.

MARZUKI NAIBAHO
Department of Physics, Universitas Indonesia, Depok, Indonesia.
Center for Advanced Materials Research (PRMM) - National Research and Innovation Agency (BRIN), Complex Puspiptek Building 440-441, Tangerang-South, Banten, Indonesia.

MASNO GINTING *
Center for Advanced Materials Research (PRMM) - National Research and Innovation Agency (BRIN), Complex Puspiptek Building 440-441, Tangerang-South, Banten, Indonesia.
*Corresponding Author Email: masn001@brin.go.id

Abstract

$MnFe_2O_4$ and $MnFe_2O_4$-Zeolite have been synthesized from sand and zeolite using the co-precipitation method for absorbing ions Pb(II) and Cu(II) in aqueous media. Samples were then characterized using SEM-EDX, XRD, VSM, BET, and AAS. The results of SEM-EDX show that the particle shape of $MnFe_2O_4$ and $MnFe_2O_4$ - zeolite is not uniform. $MnFe_2O_4$ particle size is 5-25 µm and $MnFe_2O_4$-zeolite 2-29 µm and there are impurities such as Mg, Cl, Ti, and V. XRD results confirm the presence of $MnFe_2O_4$ and other phases such as TiO_2 and SiO_2. VSM measurement shows that both $MnFe_2O_4$ and $MnFe_2O_4$-Zeolite are soft magnets with coercivity values of 302.12 Oe and 406.04 Oe consecutively. While BET analysis shows that the surface area, pore volume, and pore size of $MnFe_2O_4$ -zeolite are 222.91 m^2 /g, 0.30 cm^3 /g, and 2.70 nm larger than those of $MnFe_2O_4$. Then AAS measurement shows the optimum adsorption for Pb and Cu ions using $MnFe_2O_4$ at a dose of 100 mg/L are 96.59% and 99.24%, while for the $MnFe_2O_4$ – zeolite adsorbent for Pb ion at a dose of 100 mg/L is 96.91% and Cu ion at dose of 50 mg/L is 99.54%. In general, it was found that the adsorption percentage for both Pb and Cu ions was higher using the $MnFe_2O_4$– zeolite than the $MnFe_2O_4$.

Keywords: $MnFe_2O_4$, $MnFe_2O_4$-Zeolite, Adsorption, Co-precipitation, Heavy Metal.

Jilin Daxue Xuebao (Gongxueban)/Journal of Jilin University (Engineering and Technology Edition)
ISSN: 1671-5497
E-Publication: Online Open Access
Vol: 43 Issue: 07-2024
DOI: 10.5281/zenodo.12793416

INTRODUCTION

The lead metal ion is considered a long-term pollutant [1] and can cause organ damage even at low concentrations [2]. Not only that, lead and copper are toxic heavy metals. Lead (Pb) can cause severe kidney, liver, and reproductive system dysfunction. Copper (Cu) can cause vomiting, diarrhea, stomach cramps nausea, and even death [3][4]. Given the negative impact caused by waste metal ions Pb and Cu, it is important to purify water to remove contaminants from Pb and Cu ions[5]. Various conventional techniques can be carried out such as reverse osmosis [6], ion exchange [7], chemical precipitation [8], solvent extraction [9], etc. The adsorption method is the most appropriate method for removing heavy metal ions from water, with high effectiveness and economy [10].

Several adsorbents have been used to adsorb heavy metal ions from aqueous solutions; Namely sawdust of eucalyptus, dates, and limes [11], $\alpha - Fe_3O_4$ nanoparticles [12], bentonite[13], zeolite [14], manganese ferrite [15], zinc ferrite [16], manganese ferrite-biochar [17] and bentonite - manganese ferrite [18]. Some of these adsorbents have disadvantages such as low adsorption and difficulty in separating from the solution [19]. With the development of research on advanced materials on water pollution by heavy metals, research on manganese ferrite ($MnFe_2O_4$) adsorbents continues to grow every year. $MnFe_2O_4$ adsorbent can be used to remove heavy metal ions with magnetic separation from solution [20]. However, the $MnFe_2O_4$ adsorbent is easily agglomerated in the liquid phase, reducing the surface area and lowering the adsorption capacity. Zeolite has a larger surface area, more active sites, and high porosity which can increase the adsorption efficiency[21]. Thus, in this Article, the synthesis of $MnFe_2O_4$ and $MnFe_2O_4$ – zeolite using the co-precipitation method and their ability to absorb Pb(II) and Cu(II) metal ions from aqueous media will be reported.

MATERIALS AND METHOD

In this study, the synthesis of $MnFe_2O_4$ and $MnFe_2O_4$ – zeolite has been done using the co-precipitation method. The coprecipitation method has a simple process and can produce particles that are very small grain size and tend to be more uniform. However, the coprecipitation method will not be able to remove impurities completely. $MnCl_2$ (98%), iron sand, and clinoptilolite zeolite were used as the main precursors. Iron sand that has passed 200 mesh is dissolved using 17 ml of HCl (37%) and stirred at 500 rpm for 30 minutes at 80^{o}C, then filtered using Whatman filter paper (Grade 40 Circles). The iron sand filtrate was then mixed with $MnCl_2$ solution with a ratio of 2: 1. Furthermore, stirring was carried out with a magnetic bar at 500 rpm at room temperature until the solution became homogeneous. $MnFe_2O_4$ – zeolite was made by adding 1 gram of zeolite to the solution followed by stirring for 40 minutes at 500 rpm at room temperature. Next, the temperature of the solution was changed to 70°C before adding sodium hydroxide solution (5 mol/L) to adjust the solution pH value to 11, after which the resulting solution was stirred for 1 hour. The precipitated composite was then dried in an oven at 100°C for 24 hours. The composite was then crushed using a mortar and ready to be used as an adsorbent. The samples were then characterized using X-ray diffraction (XRD smartlab rigaku) and Scanning Electron Microscopes (SEM-EDX Hitachi SU-3500), Brunauer

Jilin Daxue Xuebao (Gongxueban)/Journal of Jilin University (Engineering and Technology Edition)
ISSN: 1671-5497
E-Publication: Online Open Access
Vol: 43 Issue: 07-2024
DOI: 10.5281/zenodo.12793416

Emmett-Teller (BET, Micrometrics ASAP 2020, USA), room temperature hysteresis loop measured by Vibrating Sample Magnetometer (VSM 250). In the batch adsorption process using a shaker carried out at optimum conditions (pH=5, T=25C, t= 60 minutes, Ci= \8mg/L)[18], [22] and the results will be tested using Atomic Absorption Spectrometry (AAS Agilent Technologies-200 series AAA/240 FS AA).

RESULTS AND DISCUSSION

Adsorbent Characterization

The surface morphology of $MnFe_2O_4$ and $MnFe_2O_4$ – zeolite adsorbents obtained from SEM-EDX measurements are shown in Figure 1.

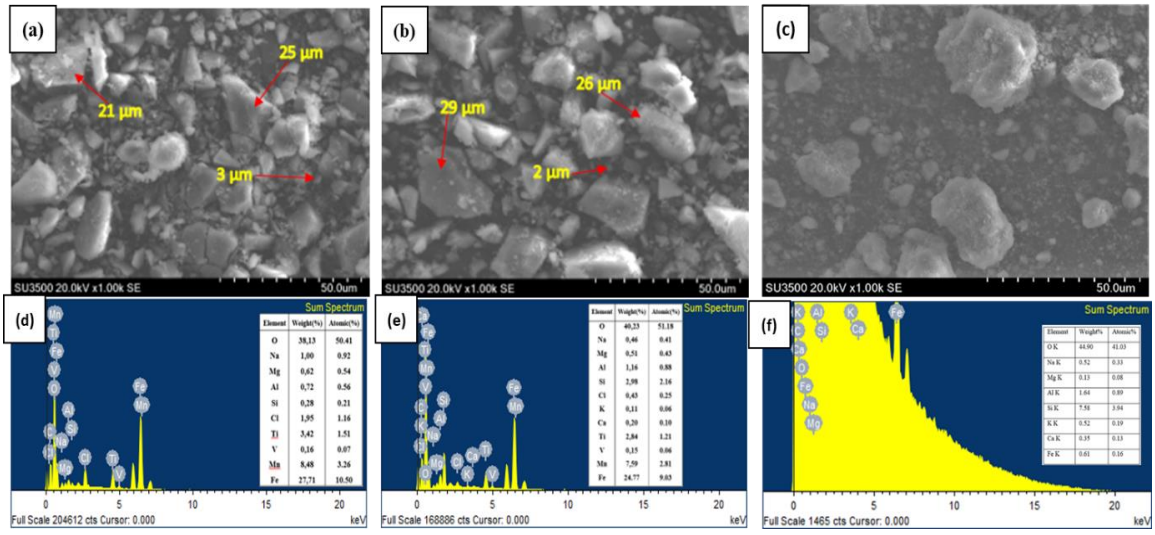

Figure 1: Surface morphology of adsorbents a) $MnFe_2O_4$, and b) $MnFe_2O_4$ – zeolite, c) Zeolite and Elemental content of adsorbents d) MnFe2O4, e) MnFe2O4 – zeolite, and f) Zeolite

Figure 1a shows that the shape of the $MnFe_2O_4$ particles is not uniform, the surface is still not uniform. The non-uniformity of the particle shape is indicated by the size range of the $MnFe_2O_4$ adsorbent particles from 3 µm to 25 µm. Particles with a large size (21 µm) experience agglomeration, because natural interactions occur between magnetic particles causing several agglomerated areas [23]. Whereas Figure 1b shows the $MnFe_2O_4$ – zeolite adsorbent also having a non-uniform particle shape and size. The particle size range of the $MnFe_2O_4$ – zeolite adsorbents is 2 µm and 29 µm. It seems that on average the particle size of $MnFe_2O_4$ – zeolite is larger than $MnFe_2O_4$

Figure 1d shows that the $MnFe_2O_4$ adsorbent has several elements such as O, Na, Mg, Al (0.72%), Si (0.28%), Cl, Ti, V, Mn, and Fe. All these elements are mostly found in all iron sands with different percentages. The highest percentage of elemental content was in the elements O, Fe, and Mn which are 38.13%, 27.71%, and 8.48% consecutively which confirmed the formation of the $MnFe_2O_4$ compound. Whereas Figure 1e shows that the content of Fe (24.77%) and Mn (7.59%) elements decreased, but the content of Al

Jilin Daxue Xuebao (Gongxueban)/Journal of Jilin University (Engineering and Technology Edition)
ISSN: 1671-5497
E-Publication: Online Open Access
Vol: 43 Issue: 07-2024
DOI: 10.5281/zenodo.12793416

(1.16%) and Si (2.98%) increased. This is due to the presence of Al and Si content in the zeolite. Other elements present in the $MnFe_2O_4$ – zeolite adsorbent are Na, Mg, Cl, K, Ca, Ti, and V. The elements Na, K, and Ca are cations from zeolite, while the presence of elements Mg, and Ti are predicted to appear from sand that was used, while Cl probably appears from the use of the HCl solvent during the synthesis process. Element V is thought to have originated from the iron sand milling process which experienced abrasion in the jar mill or ball mill.

The results of the XRD measurements of the $MnFe_2O_4$ and $MnFe_2O_4$ – zeolite samples are shown in Figure 2.

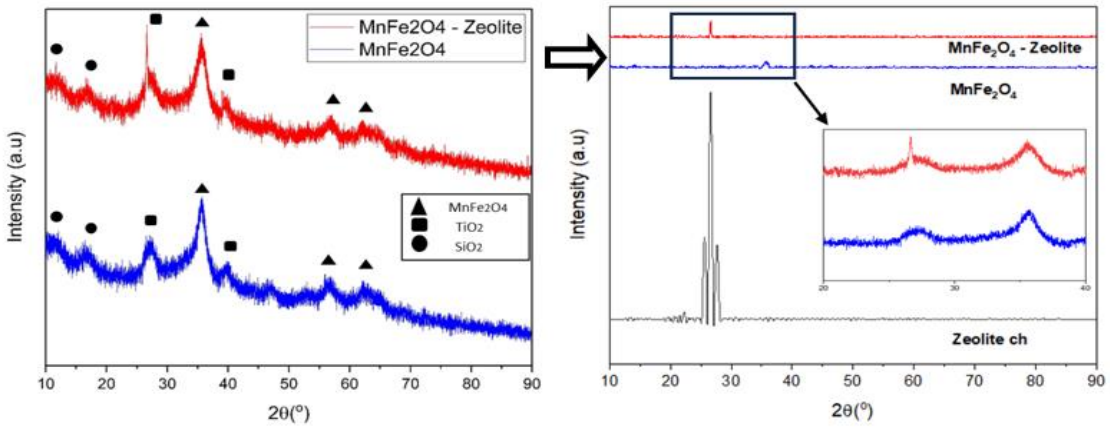

Figure 2: The pattern of diffraction peaks in $MnFe_2O_4$ and $MnFe_2O_4$ – zeolite samples

Figure 2 shows the XRD spectra for $MnFe_2O_4$ and $MnFe_2O_4$ – zeolite. It can be seen that $MnFe_2O_4$ adsorbent has several diffraction peaks with different intensities. The highest diffraction peak and several other peaks were identified phases at values 2θ of 35.57°, 46.82, 56.76° and 62.13° with hkl planes (311), (331), (511), and (440) which were matched with JCPDS data No. 73-1964 [24]. At 2θ values of 27.40° and 39.80° TiO_2 compounds were identified, while at 2θ values of 12.22° and 16.39° SiO_2 compounds were identified. The formation of TiO_2 (from iron sand) and SiO_2 (from zeolite) can seen from the presence of Ti, Si, and O elements in the sample as shown in the EDX analysis. Furthermore, in the XRD diffraction pattern of the $MnFe_2O_4$ – zeolite adsorbent, several peaks were also observed at 2θ values, they are at 12.74°, 16.37°, 20.86°, 26.57°, 35.61°, 39,46°,47, 00°, 56.88°, and 62.00°. In the analysis results, new phases appear at values of 2θ 12.74°, 16.37°, 20.86°, and 26.57° which were analyzed zeolite compounds (Hydrous sodium aluminum silicate) that were matched with JCPDS data No. 00-019-1180[25]. Analcime zeolite has the smallest pores and exhibits a compact structure. Compared to other zeolites with ideal unit cells Na16[(AlO2)16(SiO2)32].16H2O [26].

Furthermore, Figure 3 shows the hysteresis curve obtained from the VSM measurement for the $MnFe_2O_4$ and $MnFe_2O_4$ – zeolite samples.

Jilin Daxue Xuebao (Gongxueban)/Journal of Jilin University (Engineering and Technology Edition)
ISSN: 1671-5497
E-Publication: Online Open Access
Vol: 43 Issue: 07-2024
DOI: 10.5281/zenodo.12793416

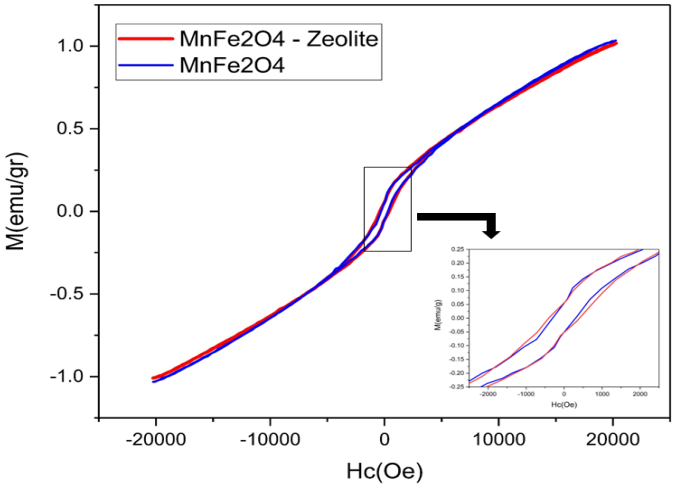

Figure 3: Hysteresis curves of adsorbents for $MnFe_2O_4$, and $MnFe_2O_4$ – zeolite

It is seen that from the shape of the hysteresis curve of the $MnFe_2O_4$ and $MnFe_2O_4$ – zeolite compounds that are shown in Fig. 3, both materials are ferrimagnetic and classified as soft-magnetic[27]. The $MnFe_2O_4$ adsorbent has a saturation magnetization value (Ms) of 1.03 emu/g, remanence magnetization (Mr) of 0.05 emu/g, and a coercivity value (Hc) of 302.12 Oe. Meanwhile, the adsorbent $MnFe_2O_4$ – zeolite has a Ms va lue of 1.02 emu/g, a Mr value of 0.06 emu/g, and an Hc value of 406.04 Oe. Based on these results, the small decrease in the Ms value for the $MnFe_2O_4$ – zeolite adsorbents is due to the zeolite being a non-magnetic material [28]. The low values of Ms, Mr, and Hc for both $MnFe_2O_4$ and $MnFe_2O_4$ – zeolite are predicted due to the presence of gangue or impurities as can be seen in the EDX and XRD results[29].

The adsorption-desorption isotherms of N2 from $MnFe_2O_4$ and $MnFe_2O_4$ – zeolite samples results that are obtained from the BET measurement are shown in Figure 4.

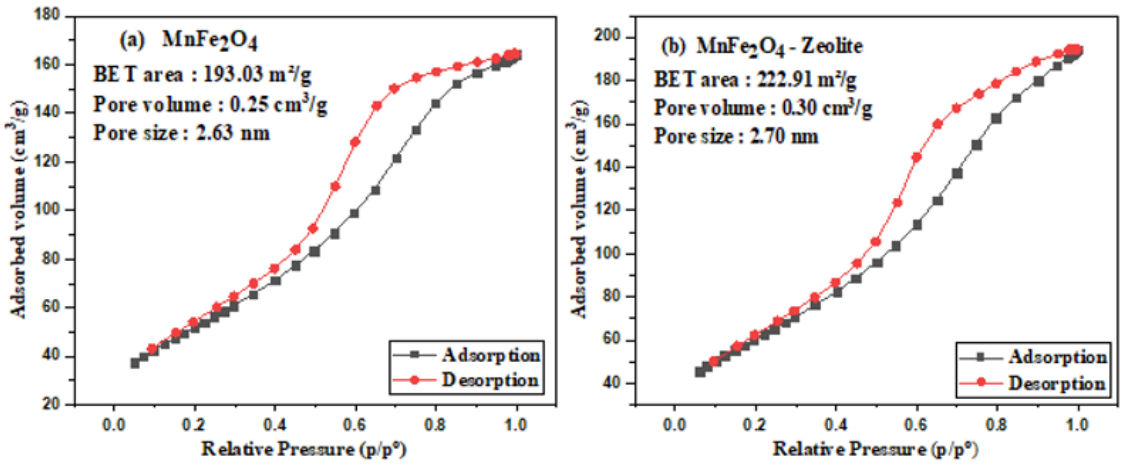

Figure 4: adsorption-desorption isotherms of N2 from adsorbents a) $MnFe_2O_4$, and b) $MnFe_2O_4$ – zeolite

Jilin Daxue Xuebao (Gongxueban)/Journal of Jilin University (Engineering and Technology Edition)
ISSN: 1671-5497
E-Publication: Online Open Access
Vol: 43 Issue: 07-2024
DOI: 10.5281/zenodo.12793416

The N2 adsorption-desorption isotherms of the two adsorbents including the type V isotherm with the H2 hysteresis loop between the adsorption and desorption curves at higher relative pressures, which shows a mesoporous surface with a complex pore structure interconnected with different sizes [30][31]. The mesoporous surface is evidenced by the pore size of the $MnFe_2O_4$ and $MnFe_2O_4$ – zeolite adsorbents, which are 2.63 nm and 2.70 nm. Differences in the shape and size of pores are caused by non-uniform particle size and shape, as shown by the SEM analysis. Calculation of the specific surface area of $MnFe_2O_4$ – zeolite (222.91 m^2/g) is much larger than that of $MnFe_2O_4$ (193.03 m^2/g), besides that the pore volume of $MnFe_2O_4$ – zeolite (0.30 cm^3/g) is larger than that of the $MnFe_2O_4$ adsorbent (0.25 cm^3/g). This is clearly due to zeolite being a material that has a high specific surface area and high porosity [32].

Adsorption of Pb and Cu

The Adsorption capacity of Pb and Cu ions by $MnFe_2O_4$ and $MnFe_2O_4$ – Zeolite adsorbents are shown in Table 1.

Table 1: The adsorption capacity of Pb and Cu ions by $MnFe_2O_4$ and $MnFe_2O_4$ – Zeolite adsorbents

Dose (mg)	pH	Contact Time (minute)	MnFe2O4						MnFe2O4 – Zeolit					
			Concentration (mg/L)				Adsorption Capacity (mg/g)		Concentration (mg/L)				Adsorption Capacity (mg/g)	
			Pb		Cu		Pb	Cu	Pb		Cu		Pb	Cu
			C_i	C_e	C_i	C_e			C_i	C_e	C_i	C_e		
50	5	60	8	0,276	8	0,061	2,57	2,44	8	0,248	8	0,037	2,58	2,65
100	5	60	8	0,273	8	0,064	3,86	3,97	8	0,261	8	0,040	3,88	3,98
150	5	60	8	0,282	8	0,069	7,72	7,94	8	0,263	8	0,047	7,74	7,96

The adsorption capacity and removal efficiency are obtained using [30]:

$$q = \frac{Ci - Ce}{w} \quad (1)$$

$$R = \frac{Ci - Ce}{Ci}\ 100\% \quad (2)$$

with: q = Adsorption capacity (mg/L), Ci = initial concentration (mg/L) Ce = Final concentration (mg/L), W = mass of magnetic powder (grams), R = Removal Efficiency (%).

As can be seen from Table 1 for $MnFe_2O_4$ the optimum adsorption capacity values were obtained at a dose of 50 mg/L for both Pb (7.72 mg/g) and Cu (7.94 mg/g) respectively. For $MnFe_2O_4$ – Zeolite also found the optimum adsorption capacity value at a dose of 50 mg/L for Pb (7.74 mg/g) and Cu (7.96 mg/g). The adsorption capacity decreased by increasing the dose in both absorbents. This is predicted due to all the active sites are completely exposed at lower doses, whereas only a small proportion of active sites are exposed at higher doses. Thus, higher adsorbent doses can cause aggregation, which decreases the total surface area of the adsorbent and causes a decrease in adsorption [33]. Another possibility could be caused by the unsaturation of adsorption sites through adsorption reactions [34].

Jilin Daxue Xuebao (Gongxueban)/Journal of Jilin University (Engineering and Technology Edition)
ISSN: 1671-5497
E-Publication: Online Open Access
Vol: 43 Issue: 07-2024
DOI: 10.5281/zenodo.12793416

The optimum adsorption capacity value obtained for $MnFe_2O_4$ – zeolite adsorbent is slightly larger compared to the $MnFe_2O_4$ adsorbent for both Pb and Cu. This is due to the addition of zeolite to the adsorbent which increases the surface area, pore volume, and pore size thereby increasing the number of active sites on the surface which can increase the adsorption capacity [21].

The Removal Efficiency of Pb(II) and Cu(II) metal ions for $MnFe_2O_4$ and $MnFe_2O_4$ -Zeolite adsorbents at pH=5, T=25C, t= 60 minutes, Ci= \8mg/L is shown in Figure 5.

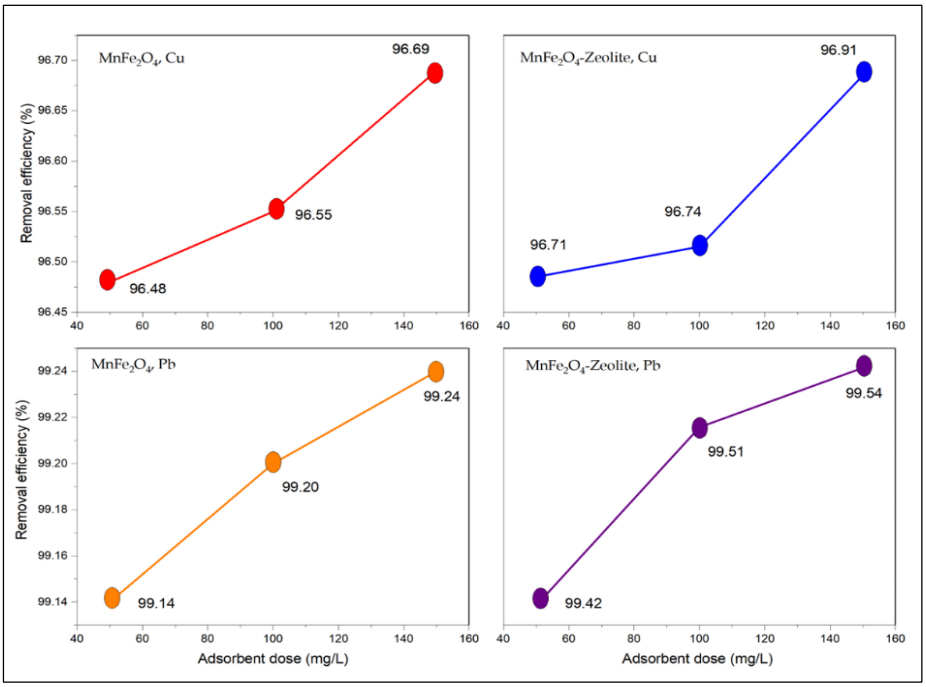

Figure 5: The Removal Efficiency of Pb(II) and Cu(II) metal ions for $MnFe_2O_4$ dan $MnFe_2O_4$ -Zeolite adsorbents

From Figure 5, It can be seen that the removal efficiency of Cu(II) ions using both $MnFe_2O_4$ and $MnFe_2O_4$ -Zeolite adsorbents is higher than the removal efficiency of Pb(II) ions. This is due to the smaller radius of Cu(II) ions (0.72 Å) compared to Pb(II) (1.29 Å) so that Cu(II) metal ions can easily occupy the adsorption active sites on the adsorbent surface [31][32]. The removal efficiency value is also increased when the adsorbent dose increases from 50, 100, and 150 mg/L. By increasing the absorbent dose, the number of active sites is also increased. Then particle aggregation will occur, which makes the adsorption efficiency of Pb and Cu increase.

The removal efficiency is also influenced by the use of absorbent pH, where if the pH used is more than 6, Pb(II) ions will precipitate in the form of hydroxide (Pb(OH)2) which will reduce the concentration of Pb ions in the solution and then decrease the removal efficiency [1]. The presence of hydron ions (H+) from the deprotonation of hydroxyl groups in water also affects the removal efficiency, where H+ ions will compete with Pb(II) and Cu(II) ions to occupy active sites on the adsorbent [33].

Jilin Daxue Xuebao (Gongxueban)/Journal of Jilin University (Engineering and Technology Edition)
ISSN: 1671-5497
E-Publication: Online Open Access
Vol: 43 Issue: 07-2024
DOI: 10.5281/zenodo.12793416

The removal efficiency of Pb and Cu ions using $MnFe_2O_4$ - zeolite is higher than $MnFe_2O_4$ adsorbent, is also due to the addition of zeolite increases the surface area, thus increasing the number of adsorption active sites on the adsorbent surface [32], and also with the presence of Na^+ cations from zeolite analcime can be exchanged with Pb^{2+} (1.29A) or Cu^{2+} (0.72A) cations [34][35]. Where the radius of Na ions is 1.02A so, the addition of zeolite increases the surface area and increases the number of active adsorption sites on the surface of the absorbent thereby increasing the absorption capacity.

In Table 2 is given the comparison of adsorption capacity with various adsorbents for Pb(II), and Cu(II)

Table: 2

No	Sample	Adsorption capacities (mg g^{-1})		ref
		Pb	Cu	
1.	chitosan/graphene oxide composites	76.9	-	[35]
2.	GO	328	-	[36]
3.	EDTA−GO	479	-	[36]
4.	EDTA−RGO	204	-	[36]
5.	amino-functionalized carbon nanotubes	58.3	-	[37]
6.	$MnFe_2O_4$ nanoparticles	488	-	[38]
7.	GO−$MnFe_2O_4$ nanohybrids	673	-	[38]
8.	Fe3O4/Cu-MOFs	219.00	-	[39]
9.	ZnO/MMT	88.50	54.06	[40]
10.	CG	16.95	6.64	[41]
11.	CG-0.5GEC	16.95	7.91	[41]
12.	CG-1.0GEC	17.01	7.54	[41]
13.	CG-2.0GEC	17.70	8.64	[41]
14.	CMS@CS	-	63.7	[42]
15.	CMS@CS-F	-	66.7	[42]
16.	PANI@APTS-Fe3O4/ATP-0.7 (288K)	265.25	180.18	[43]
17.	PANI@APTS-Fe3O4/ATP-0.7 (298K)	270.27	189.03	[43]
18.	PANI@APTS-Fe3O4/ATP-0.7 (308K)	273.22	198.80	[43]
19.	EDTA-mGO (298K)	481.2	246.1	[44]
20.	EDTA-mGO (308K)	548.1	289.4	[44]
21.	EDTA-mGO (318K)	508.4	301.2	[44]
22.	chitosan-pyromellitic dianhydride	-	66.7432	[45]
23.	CFZ10-68	109.890	57.803	[46]
24.	ZRef - FAU	103.093	57.803	[46]
25.	Oxidized MWCNT/SDBS	66.95	-	[47]
26.	Oxidized MWCNT	17.5	-	[48]
27.	Activated carbon/zeolite	549.11	-	[49]
28.	$MnFe_2O_4$	7,72	7,94	This work
29.	$MnFe_2O_4$ – Zeolite	7,74	7,96	This work

As can be seen from Table 2 the adsorption capacity of Pb and Cu by several researchers using different samples. For example, in sample CG, batch mode adsorption studies of Cu(II), Ni(II), Pb(II), and Co(II) were conducted at 25°C using 200 ml of metal ion solutions with concentrations ranging from 10-50 mg/L and 400 mg of adsorbent with an adsorption capacity of 16.95 mg/g for Pb metal and 6.64 mg/g for Cu metal [41]. Compared to the results of our research which was also conducted at 25°C using 1L water solution has a

Jilin Daxue Xuebao (Gongxueban)/Journal of Jilin University (Engineering and Technology Edition)
ISSN: 1671-5497
E-Publication: Online Open Access
Vol: 43 Issue: 07-2024
DOI: 10.5281/zenodo.12793416

fairly good adsorption capacity for $MnFe_2O_4$ absorbent of 7.72 mg/g for Pb metal and 7.94 mg/g for Cu metal. While $MnFe_2O_4$-Zeolite absorbent has an absorption capacity of 7,74 mg/g for Pb metal and 7,96 mg/g for Cu metal. The amount of both absorbents was 150 mg and the initial concentration of Pb and Cu metal was 8 mg/L as seen in Table 1. We didn't do the variation concentration in this work due to the limitations of samples of Pb and Cu Metals.

CONCLUSION

In this study, $MnFe_2O_4$ and $MnFe_2O_4$ – Zeolite were successfully synthesized from sand and zeolite using the Co-precipitation method for the use as adsorbents for the adsorption of Pb(II) and Cu(II) ions from aqueous media. The results of the SEM-EDX analysis showed that the $MnFe_2O_4$ and $MnFe_2O_4$ – zeolite particles had non-uniform particle sizes with some impurities present. XRD analysis confirmed the presence of impurities with the appearance of TiO_2 and SiO_2 peaks. Both adsorbents are ferrimagnetic and show soft magnet behavior with a coercivity value of $MnFe_2O_4$ – zeolite is larger than $MnFe_2O_4$. The BET analysis also showed that the surface area, pore volume, and pore size of the $MnFe_2O_4$ -zeolite adsorbent are larger than the $MnFe_2O_4$ adsorbents. From the adsorption test with the influence of the adsorbent dose, there was an increase in the percentage of optimum adsorption on Pb and Cu by using the $MnFe_2O_4$ - zeolite adsorbent. From this study, it is found that $MnFe_2O_4$ – zeolite is a very effective absorbent in removing the Cu and Pb ions from the water solution.

Acknowledgments

The research/publication of this article was the collaboration between the National Research and Innovation Agency (BRIN) and Universitas Sriwijaya, and part is funded by DIPA of Public Service Agency of Universitas Sriwijaya 2023. Nomor SP DIPA-023.17.2.677515/2023, On November 30, 2022. By the Rector's Decree Number: 0188/UN9.3.1/SK/2023, On April 18, 2023

References

1) M. R. Hassan and M. I. Aly, "Magnetically Synthesized MnFe2O4 Nanoparticles as an Effective Adsorbent for Lead Ions Removal from an Aqueous Solution," *Aqua Water Infrastructure, Ecosyst. Soc.*, vol. 70, no. 6, pp. 901–920, 2021, doi: 10.2166/aqua.2021.132.

2) R. Bhateria and R. Singh, "A Review on Nanotechnological Application of Magnetic Iron Oxides for Heavy Metal Removal," *J. Water Process Eng.*, vol. 31, no. October 2018, p. 100845, 2019, doi: 10.1016/j.jwpe.2019.100845.

3) Z. Bonyadi *et al.*, "Ultrasonic-assisted synthesis of Populus alba activated carbon for water defluorination: Application for real wastewater," *Korean J. Chem. Eng.*, vol. 36, no. 10, pp. 1595–1603, 2019, doi: 10.1007/s11814-019-0373-0.

4) E. N. Zare, A. Motahari, and M. Sillanpää, "Nanoadsorbents Based on Conducting Polymer Nanocomposites with Main Focus on Polyaniline and its Derivatives for Removal of Heavy Metal Ions/Dyes: A Review," *Environ. Res.*, vol. 162, pp. 173–195, 2018, doi: 10.1016/j.envres.2017.12.025.

5) S. Ghezelbash, M. Yousefi, M. Hossainisadr, and S. Baghshahi, "Structural and Magnetic Properties of Sn4+ Doped Strontium Hexaferrites Prepared via Sol–Gel Auto-Combustion Method," *IEEE Trans. Magn.*, pp. 1–6, 2018, doi: 10.1109/TMAG.2018.2844364.

ISSN: 1671-5497
E-Publication: Online Open Access
Vol: 43 Issue: 07-2024
DOI: 10.5281/zenodo.12793416

6) B. S. Thaçi and S. T. Gashi, “Reverse Osmosis Removal of Heavy Metals from Wastewater Effluents Using Biowaste Materials Pretreatment,” *Polish J. Environ. Stud.*, vol. 28, no. 1, pp. 337–341, 2019, doi: 10.15244/pjoes/81268.

7) L. Dong, L. Hou, Z. Wang, P. Gu, G. Chen, and R. Jiang, “A New Function of Spent Activated Carbon in BAC Process: Removing Heavy Metals by Ion Exchange Mechanism,” *J. Hazard. Mater.*, vol. 359, pp. 76–84, 2018, doi: 10.1016/j.jhazmat.2018.07.030.

8) Y. Zhang and X. Duan, “Chemical Precipitation of Heavy Metals from Wastewater by Using the Synthetical Magnesium Hydroxy Carbonate,” *Water Sci. Technol.*, vol. 81, no. 6, pp. 1130–1136, 2020, doi: 10.2166/wst.2020.208.

9) Y. J. Shih, S. K. Chien, S. R. Jhang, and Y. C. Lin, “Chemical Leaching, Precipitation, and Solvent Extraction for Sequential Separation of Valuable Metals in Cathode Material of Spent Lithium Ion Batteries,” *J. Taiwan Inst. Chem. Eng.*, vol. 100, pp. 151–159, 2019, doi: 10.1016/j.jtice.2019.04.017.

10) R. Hasanzadeh, P. N. Moghadam, N. Bahri-Laleh, and M. Sillanpää, *Effective removal of toxic metal ions from aqueous solutions: 2- Bifunctional magnetic nanocomposite base on novel reactive PGMA-MAn copolymer@Fe3O4 nanoparticles*, vol. 490. Elsevier Inc., 2017. doi: 10.1016/j.jcis.2016.11.098.

11) H. Esmaeili and R. Foroutan, “Adsorptive Behavior of Methylene Blue onto Sawdust of Sour Lemon, Date Palm, and Eucalyptus as Agricultural Wastes,” *J. Dispers. Sci. Technol.*, vol. 40, no. 7, pp. 990–999, 2019, doi: 10.1080/01932691.2018.1489828.

12) M. Rincón Joya, J. Barba Ortega, J. O. D. Malafatti, and E. C. Paris, “Evaluation of Photocatalytic Activity in Water Pollutants and Cytotoxic Response of α-Fe2O3 Nanoparticles,” *ACS Omega*, vol. 4, no. 17, pp. 17477–17486, 2019, doi: 10.1021/acsomega.9b02251.

13) J. Y. Jo, J. H. Choi, Y. F. Tsang, and K. Baek, “Pelletized Adsorbent of Alum Sludge and Bentonite for Removal of Arsenic,” *Environ. Pollut.*, vol. 277, p. 116747, 2021, doi: 10.1016/j.envpol.2021.116747.

14) Y. Kobayashi, F. Ogata, T. Nakamura, and N. Kawasaki, “Synthesis of Novel Zeolites Produced from fly Ash by Hydrothermal Treatment in Alkaline Solution and its Evaluation as an Adsorbent for Heavy Metal Removal,” *J. Environ. Chem. Eng.*, vol. 8, no. 2, p. 103687, 2020, doi: 10.1016/j.jece.2020.103687.

15) S. Martinez–Vargas *et al.*, “As(III) and As(V) Adsorption on Manganese Ferrite Nanoparticles,” *J. Mol. Struct.*, vol. 1154, no. Iii, pp. 524–534, 2018, doi: 10.1016/j.molstruc.2017.10.076.

16) F. Fajardo, I. D. Susilowati, Nazriati, Sumari, and A. Nur, “Synthesis of ZnFe2O4 Nanoparticles with PEG 6000 and Their Potential Application for Adsorbent,” *IOP Conf. Ser. Mater. Sci. Eng.*, vol. 515, no. 1, pp. 1–9, 2019, doi: 10.1088/1757-899X/515/1/012049.

17) Z. Xu *et al.*, “Manganese Ferrite Modified Biochar from Vinasse for Enhanced Adsorption of Levofloxacin: Effects and Mechanisms,” *Environ. Pollut.*, vol. 272, p. 115968, 2021, doi: 10.1016/j.envpol.2020.115968.

18) A. Ahmadi, R. Foroutan, H. Esmaeili, and S. Tamjidi, “The role of bentonite clay and bentonite clay@MnFe2O4 composite and their physicochemical properties on the removal of Cr(III) and Cr(VI) from aqueous media,” *Environ. Sci. Pollut. Res.*, vol. 27, no. 12, pp. 14044–14057, 2020, doi: 10.1007/s11356-020-07756-x.

19) R. Wang, R. Liang, T. Dai, J. Chen, X. Shuai, and C. Liu, “Pectin-Based Adsorbents for Heavy Metal Ions: A Review,” *Trends Food Sci. Technol.*, vol. 91, no. May 2018, pp. 319–329, 2019, doi: 10.1016/j.tifs.2019.07.033.

20) N. Akhlaghi and G. Najafpour-Darzi, “Manganese Ferrite (MnFe2O4) Nanoparticles: From Synthesis to Application -A Review,” *J. Ind. Eng. Chem.*, vol. 103, pp. 292–304, 2021, doi: 10.1016/j.jiec.2021.07.043.

ISSN: 1671-5497
E-Publication: Online Open Access
Vol: 43 Issue: 07-2024
DOI: 10.5281/zenodo.12793416

21) A. Amrollahi, M. Massinaei, and A. Z. Moghaddam, “Removal of the residual xanthate from flotation plant tailings using bentonite modified by magnetic nano-particles,” *Miner. Eng.*, vol. 134, no. January, pp. 142–155, 2019, doi: 10.1016/j.mineng.2019.01.031.

22) Y. Zhao, Q. Li, H. Ren, and R. Zhou, “Activation of persulfate by magnetic MnFe2O4-bentonite for catalytic degradation of 2,4-dichlorophenol in aqueous solutions,” *Chem. Res. Chinese Univ.*, vol. 33, no. 3, pp. 415–421, 2017, doi: 10.1007/s40242-017-6485-3.

23) M. A. S. Amulya, H. P. Nagaswarupa, M. R. A. Kumar, C. R. Ravikumar, and K. B. Kusuma, “Sonochemical Synthesis of MnFe2O4 Nanoparticles and their Electrochemical and Photocatalytic Properties,” *J. Phys. Chem. Solids*, vol. 148, no. August 2020, p. 109661, 2021, doi: 10.1016/j.jpcs.2020.109661.

24) D. K. Mondal, C. Borgohain, N. Paul, and J. P. Borah, “Tuning hyperthermia efficiency of MnFe2O4/ZnS nanocomposites by controlled ZnS concentration,” *J. Mater. Res. Technol.*, vol. 8, no. 6, pp. 5659–5670, 2019, doi: 10.1016/j.jmrt.2019.09.034.

25) D. Novembre and D. Gimeno, “Synthesis and Characterization of Analcime (ANA) Zeolite using a Kaolinitic rock,” *Sci. Rep.*, vol. 11, no. 1, pp. 1–9, 2021, doi: 10.1038/s41598-021-92862-0.

26) H. R. Bortolini, D. S. Lima, and O. W. Perez-Lopez, “Hydrothermal synthesis of analcime without a template,” *J. Cryst. Growth*, vol. 532, no. November 2019, p. 125424, 2020, doi: 10.1016/j.jcrysgro.2019.125424.

27) R. Nisticò, F. Cesano, and F. Garello, *Magnetic materials and systems: Domain structure visualization and other characterization techniques for the application in the materials science and biomedicine*, vol. 8, no. 1. 2020. doi: 10.3390/inorganics8010006.

28) S. Gautam *et al.*, “Superparamagnetic MnFe2O4 Dispersed Over Graphitic Carbon Sand Composite and Bentonite as Magnetically Recoverable Photocatalyst for Antibiotic Mineralization,” *Sep. Purif. Technol.*, vol. 172, pp. 498–511, 2017, doi: 10.1016/j.seppur.2016.09.006.

29) M. Zheng, X. C. Wu, B. S. Zou, and Y. J. Wang, “Magnetic properties of nanosized MnFe2O4 particles,” *J. Magn. Magn. Mater.*, vol. 183, no. 1–2, pp. 152–156, 1998, doi 10.1016/S0304-8853(97)01057-3.

30) E. Barsotti, S. P. Tan, M. Piri, and J. H. Chen, “Capillary-condensation hysteresis in naturally-occurring nanoporous media,” *Fuel*, vol. 263, no. August, p. 116441, 2020, doi: 10.1016/j.fuel.2019.116441.

31) R. Bardestani, G. S. Patience, and S. Kaliaguine, “Experimental methods in chemical engineering: specific surface area and pore size distribution measurements—BET, BJH, and DFT,” *Can. J. Chem. Eng.*, vol. 97, no. 11, pp. 2781–2791, 2019, doi: 10.1002/cjce.23632.

32) H. Duan, X. Hu, and Z. Sun, “Magnetic zeolite imidazole framework material-8 as an effective and recyclable adsorbent for removal of ceftazidime from aqueous solution,” *J. Hazard. Mater.*, vol. 384, no. October 2019, p. 121406, 2020, doi: 10.1016/j.jhazmat.2019.121406.

33) F. Y. Wang, H. Wang, and J. W. Ma, “Adsorption of cadmium (II) ions from aqueous solution by a new low-cost adsorbent-Bamboo charcoal,” *J. Hazard. Mater.*, vol. 177, no. 1–3, pp. 300–306, 2010, doi: 10.1016/j.jhazmat.2009.12.032.

34) A. A. Alghamdi, A. B. Al-Odayni, W. S. Saeed, A. Al-Kahtani, F. A. Alharthi, and T. Aouak, “Efficient adsorption of lead (II) from aqueous phase solutions using polypyrrole-based activated carbon,” *Materials (Basel).*, vol. 12, no. 12, 2019, doi: 10.3390/ma12122020.

35) L. Fan, C. Luo, M. Sun, X. Li, and H. Qiu, “Highly selective adsorption of lead ions by water-dispersible magnetic chitosan/graphene oxide composites,” *Colloids Surfaces B Biointerfaces*, vol. 103, pp. 523–529, 2013, doi: 10.1016/j.colsurfb.2012.11.006.

ISSN: 1671-5497
E-Publication: Online Open Access
Vol: 43 Issue: 07-2024
DOI: 10.5281/zenodo.12793416

36) C. J. Madadrang *et al.*, “Adsorption behavior of EDTA-graphene oxide for Pb (II) removal,” *ACS Appl. Mater. Interfaces*, vol. 4, no. 3, pp. 1186–1193, 2012, doi: 10.1021/am201645g.

37) G. D. Vuković *et al.*, “Removal of lead from water by amino modified multi-walled carbon nanotubes,” *Chem. Eng. J.*, vol. 173, no. 3, pp. 855–865, 2011, doi: 10.1016/j.cej.2011.08.036.

38) K. A. Mangai, P. Sureshkumar, M. Priya, and M. Rathnakumari, “Structural and Magnetic properties of Strontium Hexa-Ferrites for Permanent Magnets,” *Int. J. Sci. Eng. Res.*, vol. 5, no. 3, pp. 65–69, 2014.

39) Z. Shi *et al.*, “Magnetic metal-organic frameworks (MOFs) composite for removal of lead and malachite green in wastewater,” *Colloids Surfaces A Physicochem. Eng. Asp.*, vol. 539, no. 2010, pp. 382–390, 2018, doi 10.1016/j.colsurfa.2017.12.043.

40) H. A. Sani, M. B. Ahmad, M. Z. Hussein, N. A. Ibrahim, A. Musa, and T. A. Saleh, “Nanocomposite of ZnO with montmorillonite for removal of lead and copper ions from aqueous solutions,” *Process Saf. Environ. Prot.*, vol. 109, pp. 97–105, 2017, doi: 10.1016/j.psep.2017.03.024.

41) M. Osińska, “Removal of lead(II), copper(II), cobalt(II) and nickel(II) ions from aqueous solutions using carbon gels,” *J. Sol-Gel Sci. Technol.*, vol. 81, no. 3, pp. 678–692, 2017, doi: 10.1007/s10971-016-4256-0.

42) L. T. Zhang *et al.*, “Low-Cost magnetic adsorbent for efficient Cu(II) removal from water,” *Mater. Res. Express*, vol. 7, no. 10, 2020, doi: 10.1088/2053-1591/abbe3f.

43) P. Sun, W. Zhang, B. Zou, X. Wang, L. Zhou, and Z. Ye, “Applied Clay Science Efficient adsorption of Cu (II), Pb (II) and Ni (II) from wastewater by PANI @ APTS-magnetic attapulgite composites,” vol. 209, no. January, 2021.

44) L. Cui *et al.*, “EDTA functionalized magnetic graphene oxide for removal of Pb(II), Hg(II) and Cu(II) in water treatment: Adsorption mechanism and separation property,” *Chem. Eng. J.*, vol. 281, pp. 1–10, 2015, doi: 10.1016/j.cej.2015.06.043.

45) J. Deng *et al.*, “Competitive adsorption of Pb(II), Cd(II) and Cu(II) onto chitosan-pyromellitic dianhydride modified biochar,” *J. Colloid Interface Sci.*, vol. 506, pp. 355–364, 2017, doi: 10.1016/j.jcis.2017.07.069.

46) I. V. Joseph, L. Tosheva, and A. M. Doyle, “Simultaneous removal of Cd(II), Co(II), Cu(II), Pb(II), and Zn(II) ions from aqueous solutions via adsorption on FAU-type zeolites prepared from coal fly ash,” *J. Environ. Chem. Eng.*, vol. 8, no. 4, p. 103895, 2020, doi: 10.1016/j.jece.2020.103895.

47) J. Li, S. Chen, G. Sheng, J. Hu, X. Tan, and X. Wang, “Effect of surfactants on Pb(II) adsorption from aqueous solutions using oxidized multiwall carbon nanotubes,” *Chem. Eng. J.*, vol. 166, no. 2, pp. 551–558, 2011, doi: 10.1016/j.cej.2010.11.018.

48) X. Ren *et al.*, “Comparative study of Pb(II) sorption on XC-72 carbon and multi-walled carbon nanotubes from aqueous solutions,” *Chem. Eng. J.*, vol. 170, no. 1, pp. 170–177, 2011, doi: 10.1016/j.cej.2011.03.050.

49) V. K. Jha, M. Matsuda, and M. Miyake, “Sorption properties of the activated carbon-zeolite composite prepared from coal fly ash for Ni2+, Cu2+, Cd2+ and Pb2+,” *J. Hazard. Mater.*, vol. 160, no. 1, pp. 148–153, 2008, doi: 10.1016/j.jhazmat.2008.02.107.